The Journal of Infectious Diseases

MAJOR ARTICLE

Is Cellular Senescence a Biological Feature of Long COVID? A Transcriptomic Analysis Across Comparative Postacute Sequelae Phenotypes

Nusrat J. Epsi,[1,2] Stephanie A. Richard,[1,2] Michael J. Morris,[3] David A. Lindholm,[3,4] Anuradha Ganesan,[1,2,5] Rhonda E. Colombo,[1,2,4,6] Katrin Mende,[1,2,3] Milissa U. Jones,[7] Allison M. W. Malloy,[7] Leah H. Rubin,[8,9] Brian K. Agan,[1,2] David R. Tribble,[1] Timothy H. Burgess,[1] Clifton Dalgard,[10] Michael A. Puskarich,[11] and Simon D. Pollett[1,2]

[1]Infectious Disease Clinical Research Program, Department of Preventive Medicine and Biostatistics, Uniformed Services University of the Health Sciences, Bethesda, Maryland, USA; [2]The Henry M. Jackson Foundation for the Advancement of Military Medicine, Inc., Bethesda, Maryland, USA; [3]Joint Base San Antonio-Fort Sam, Brooke Army Medical Center, Houston, Texas, USA; [4]Department of Medicine, Uniformed Services University of the Health Sciences, Bethesda, Maryland, USA; [5]Division of Infectious Diseases, Walter Reed National Military Medical Center, Bethesda, Maryland, USA; [6]Division of Infectious Diseases, Madigan Army Medical Center, Joint Base Lewis McChord, Fort Lewis, Washington, USA; [7]Department of Pediatrics, Uniformed Services University of the Health Sciences, Bethesda, Maryland, USA; [8]Department of Neurology, Psychiatry and Behavioral Sciences, Molecular and Cellular Pathobiology, School of Medicine, Johns Hopkins University, Baltimore, Maryland, USA; [9]Department of Epidemiology, Bloomberg School of Public Health, Johns Hopkins University, Baltimore, Maryland, USA; [10]Department of Anatomy, Physiology and Genetics, Uniformed Services University, Bethesda, Maryland, USA; and [11]Department of Emergency Medicine, University of Minnesota, Minneapolis, Minnesota, USA

Background. Cellular senescence, involving cell-cycle arrest and inflammatory factor release, may play a role in Long COVID development. We investigated the role of senescence-associated genes across multiple postacute sequelae phenotypes.

Methods. Participants from a cohort study were grouped into post-COVID-19 groups: (1) sensory, fatigue/difficulty thinking, and difficulty breathing/exercise intolerance, identified through a machine learning analysis of symptom data; (2) cognitive impairment, measured using a screening cognitive assessment tool (BRACE); and (3) persistent dyspnea, identified using a symptom-scale known to correlate with a 6-minute-walk-test. Postinfection whole-blood samples underwent transcriptomic analysis with 47 125 genes used as the reference signature for gene set enrichment analysis against the SenMayo cellular-senescence query gene set (n = 125); enrichment were based on normalized enrichment scores (NES).

Results. SenMayo genes were significantly upregulated in the early postinfection period in (1) 56 individuals who subsequently developed Long COVID symptom phenotypes, compared to 104 who did not develop Long COVID symptoms (NES = 6.04, $P = .001$); (2) 32 individuals with long-term cognitive impairment compared with 40 without long-term cognitive impairment measured by BRACE (NES = 2.58, $P = .032$); and (3) 26 participants who had persistent dyspnea compared with 53 without persistent dyspnea measured by the validated dyspnea instrument (NES = 6.29, $P = .001$). *ETS2* was upregulated across all impairment-related phenotypes, while other SenMayo genes showed phenotype-specific variability.

Conclusions. This study suggests a role of senescence-associated genes in the development of Long COVID, including shared and unique transcriptomic patterns across phenotypes.

Keywords. postacute sequelae; COVID-19; SARS-CoV-2; cellular senescence; SenMayo.

Long COVID represents a spectrum of symptoms that persist beyond acute illness [1]. Manifestations include cognitive, cardiopulmonary, and systemic fatigue symptoms, among others, contributing to morbidity and impaired quality of life [1]. Despite extensive efforts to investigate its underlying mechanisms, the heterogeneity of Long COVID phenotypes poses a challenge to understand the underlying pathophysiology.

One emerging hypothesis suggests that cellular senescence-associated biological processes and transcriptional programs may contribute to the pathogenesis of Long COVID [2–4]. Cellular senescence is defined as a stable cell-cycle arrest in response to physiological stressors such as DNA damage, mitochondrial dysfunction, or chronic inflammation [5]. This process is largely mediated by key pathways, including *p53/p21* and $p16^{INK4a/Rb}$, which regulate cell proliferation and survival [6–8].

Senescent cells are metabolically active and secrete a repertoire of proinflammatory cytokines, chemokines, and matrix-degrading

Received 03 December 2025; accepted 12 June 2026; published online 24 June 2026

Correspondence: Nusrat J. Epsi, PhD, HJF for the Infectious Disease Clinical Research Program, Department of Preventive Medicine and Biostatistics, Uniformed Services University of the Health Sciences, 6720A Rockledge Drive, Suite 250, Bethesda, MD 20817 (nepsi@idcrp.org); Simon D. Pollett, MBBS, HJF for the Infectious Disease Clinical Research Program, Department of Preventive Medicine and Biostatistics, Uniformed Services University of the Health Sciences, 6720A Rockledge Drive, Suite 250, Bethesda, MD 20817 (spollett@idcrp.org).

The Journal of Infectious Diseases® 2026;234:e869–80

© The Author(s) 2026. Published by Oxford University Press on behalf of Infectious Diseases Society of America.

This is an Open Access article distributed under the terms of the Creative Commons Attribution-NonCommercial-NoDerivs licence (https://creativecommons.org/licenses/by-nc-nd/4.0/), which permits non-commercial reproduction and distribution of the work, in any medium, provided the original work is not altered or transformed in any way, and that the work is properly cited. For commercial re-use, please contact reprints@oup.com for reprints and translation rights for reprints. All other permissions can be obtained through our RightsLink service via the Permissions link on the article page on our site—for further information please contact journals.permissions@oup.com.

https://doi.org/10.1093/infdis/jiag315

Downloaded from academic.oup.com/jid/article/234/4/e869/8713052 by guest on 18 October 2026

proteins, collectively referred to as the senescence-associated secretory phenotype (SASP) [9–13]. While cellular senescence plays an essential role in tissue repair and immune surveillance, the persistent accumulation of senescent cells in aging tissues is associated with chronic inflammation, tissue dysfunction, and age-related diseases, such as cardiovascular disease, neurodegeneration, and immune aging (immunosenescence) [14, 15]. Senescent cells can also disrupt the balance of innate and adaptive immunity, particularly impacting T cells and B cells, which are crucial for immune resilience and recovery [16]. Recent studies have identified biomarkers of cellular senescence in $CD3^+$ T cells, as well as plasma proteins [17]. These SASP-associated biomarkers not only reflect senescent cell burden but also contribute to systemic inflammation and immune dysregulation [18].

To quantify cellular senescence, the SenMayo gene set has been developed and validated using a combination of bulk tissue, single-cell, cross-species, and intervention-based analyses [17]. These transcriptomic signatures provide a validated approach for assessing senescence-associated transcriptional programs in both tissue and blood samples [17], enabling investigation of senescence-related biology across a variety of disease states. Emerging evidence suggests that viral infections, including SARS-CoV-2, can accelerate cellular senescence [19], including in human cases and preclinical models [19, 20].

While cellular senescence postacute COVID-19 is increasingly well described, the contribution of post-SARS-CoV-2 cellular senescence to Long COVID remains poorly understood. Given the persistent inflammatory state observed in some Long COVID studies [21–23], it is plausible that senescence-associated and inflammatory pathways contribute to tissue dysfunction and clinical phenotypes of Long COVID [19]. However, whether senescence is a predictor or mechanistic driver of Long COVID pathogenesis remains unclear.

In this study, we aimed to explore the relationship between early postinfection senescence-associated transcriptional signatures and the subsequent development of Long COVID by leveraging transcriptomic analysis of whole-blood samples. We utilized the SenMayo gene set [17] to identify putative molecular pathways associated with senescence in individuals following SARS-CoV-2 infection. Due to the heterogeneity of Long COVID clinical presentations, we explore the association of cellular-senescence biomarkers with participant-reported symptom-based phenotypes, in addition to objectively evaluated cognitive and cardiopulmonary phenotypes.

METHODS

Study Population and General Study Design

This study utilizes data from the Epidemiology, Immunology, and Clinical Characteristics of Emerging Infectious Diseases with Pandemic Potential (EPICC) longitudinal cohort study, which investigates COVID-19 outcomes in military health system (MHS) beneficiaries [24–26]. EPICC enrolled participants from March 2020 to May 2022, including individuals with confirmed SARS-CoV-2 infection, COVID-19-like symptoms, and high-risk exposures, with later expansion to COVID-19 vaccinated individuals. Participants were followed at predefined intervals with prospective collection of data and specimens (Supplementary Table 1).

Upper respiratory tract swabs were collected for SARS-CoV-2 detection by RT-PCR. For host response analyses, whole-blood samples were collected, including PAXgene Blood RNA tubes that were processed for transcriptomic profiling. As outlined in Supplementary Table 1, PAXgene whole-blood RNA collection only took place up to Day 28 postenrollment. These molecular data were integrated with clinical metadata, including vaccination status, comorbidities, and acute COVID-19 severity. Relevant clinical information was abstracted from the MHS data repository and supplemented by structured questionnaires.

Approach to Comparative Long COVID Phenotyping

EPICC enrollment afforded several approaches to phenotyping Long COVID (Supplementary Figure 1): (1) chronic self-reported postinfectious symptom patterns defined by machine learning (ML) based cluster analyses, as described in [27]; (2) objective measurement of cognitive impairment via a participant operated mobile app, as described in [28]; and (3) self-reported dyspnea by a standardized 12-point dyspnea questionnaire, which we previously demonstrated correlated with impaired 6-minute-walk-test (6MWT) scores [29]. In each phenotyping approach, we included 2 comparison groups: (1) SARS-CoV-2 positive controls without post-SARS-CoV-2 sequelae, and (2) SARS-CoV-2 negative participants. For each phenotype, RNA sequencing was performed on a subset of participants, based on the availability of appropriately collected and stored PAXgene blood samples at the time of analysis.

ML Defined Symptom-based Long COVID Phenotyping

To classify participants based on Long COVID symptoms, a ML approach was applied to participant-reported symptom data [27] (Supplementary Materials). Analyses were additionally restricted to participants younger than 65 years of age with no existing comorbidities to reduce potential confounding from age-related and baseline comorbidity-associated symptom burden. This analysis identified 3 distinct Long COVID phenotypes: (1) sensory symptoms (eg, loss of taste and/or smell), (2) fatigue/difficulty thinking, and (3) exercise intolerance or difficulty breathing (Supplementary Figure 2). This classification framework has previously been shown to recapitulate ML-based symptom clusters in the RECOVER observational cohort [27, 30].

Downloaded from academic.oup.com/jid/article/234/4/e869/8713052 by guest on 18 October 2026

Long COVID Cognitive Phenotyping

Cognitive impairment was assessed among both SARS-CoV-2 infected and uninfected EPICC participants using the Brain Baseline Assessment of Cognition and Everyday Functioning (BRACE), a validated app-based cognitive testing platform which screens for cognitive impairment [28]. Assessment was conducted postinfection for SARS-CoV-2 positive individuals (Supplementary Material). These assessments extended prior subjective cognitive evaluations conducted in the EPICC study [31]. Briefly, cognitive function was evaluated across multiple domains, including psychomotor speed, executive function and mental flexibility, processing speed and interference resolution, and visuospatial memory.

Cardiopulmonary Long COVID Phenotyping

Cardiopulmonary complications of COVID-19 were investigated using data from the chronic impairment with pulmonary symptoms (ChIPS) EPICC substudy [29] (Supplementary Materials). Briefly, this substudy enrolled participants with and without chronic dyspnea 3 months post-COVID-19 infection. All participants underwent comprehensive cardiopulmonary assessments, including high-resolution CT scans, echocardiograms (echo), pulmonary function tests, electrocardiograms, and 6MWT.

Negative Controls

We further compared transcriptomic profiles of SARS-CoV-2 positive participants (with and without Long COVID) to a SARS-CoV-2 negative-control group (Supplementary Materials). Here, we restricted SARS-CoV-2 negative control set to younger individuals with no reported comorbidities and ensured that controls were matched by sample collection timeframes, reducing variation unrelated to infection status.

RNA Sequencing

RNA sequencing was performed on EPICC participants from postinfection SARS-CoV-2 PAXgene blood specimens. Additionally, we leveraged transcriptomic data generated from early postinfection time points (samples collected within the initial phase following SARS-CoV-2 infection, typically within a median of 4 weeks postinfection) in a subset of convenience-sampled participants without Long COVID, as well as from a convenience-sampled group of SARS-CoV-2 negative participants. Additional details are provided in the Supplementary Materials.

SenMayo Gene Set

SenMayo gene set comprises 125 genes associated with cellular senescence [17], organized into functional categories including metalloproteases, cytokines and chemokines, intercellular signaling molecules, transmembrane receptors, protease inhibitors, and growth factors [17] (Supplementary Table 2).

Transcriptomic and Statistical Analysis

Raw RNA-seq count data were normalized and analyzed using DESeq2 [32] to identify differentially expressed genes (DEGs) based on the negative binomial distribution. DEGs were identified by comparing experimental conditions, with statistical significance determined using the Benjamini–Hochberg false discovery rate (FDR) correction. Genes with an adjusted P value (FDR) < .05 were considered significant.

To better understand the cellular composition underlying transcriptional changes, we performed cell-type deconvolution using the EPIC (estimating the proportion of immune and cancer cells) tool [33] allowing estimation of immune and stromal cell proportions across Long COVID phenotypes.

To identify cellular-senescence genes that contribute to Long COVID, gene set enrichment analysis (GSEA) [34] was performed using the SenMayo gene set as the query, and RNA-Seq expressional profiles for each Long COVID phenotype as the reference signature, with enrichment significance assessed after FDR adjustment for multiple testing (Supplementary Figure 3). Enrichment was assessed based on normalized enrichment scores (NES) and statistical significance, enabling the identification of senescence-associated processes relevant to Long COVID. Descriptive statistics were calculated to summarize demographic and clinical characteristics of the study populations, with P values determined using Fisher's exact test. All figures and statistical analyses were performed in R version 4·0·2 [35].

Ethics

This study was approved by the Uniformed Services University of the Health Sciences (USUHS) Institutional Review Board (IRB) under protocol IDCRP-085 [24]; all participants or their legally authorized representative provided informed consent to participate.

RESULTS

Demographic, Clinical Characteristics, and Long COVID Phenotyping Results Among Those With RNA-Seq Data Available

Among 7911 participants enrolled in the EPICC study, 17% of adult participants underwent RNA sequencing of whole-blood samples (Supplementary Figure 1). This analysis focuses on 3 Long COVID phenotypes: ML-based symptom groups [27], cognitive outcomes from the BRACE substudy [28], and cardiopulmonary outcomes from the ChIPS substudy [29]. For each of these phenotypes, we compared transcriptomic profiles to a common SARS-CoV-2 negative-control group (Table 1).

In the ML-based symptom phenotyping analysis, RNA sequencing was performed on 160 participants with and without moderate–severe symptoms at 3–9 months post-COVID-19. These participants were categorized into 4 distinct clusters [27]: sensory symptoms (n = 12), characterized by loss of taste and/or smell; fatigue/difficulty thinking (n = 17), associated

Downloaded from academic.oup.com/jid/article/234/4/e869/8713052 by guest on 18 October 2026

Table 1. Clinical and Demographic Characteristics of Selected EPICC Participants

	Participants With ML Symptom-based Phenotyping[a] (N = 160)	Participants With Cognitive Phenotyping (BRACE[b]) (N = 72)	Participants With Cardiopulmonary Phenotyping (ChIPS[c]) (N = 79)	Controls (N = 40)	Total (N = 351)	*P* Value[d]
Age group						<.01
18–44	140 (87.5%)	42 (58.3%)	35 (44.3%)	36 (90.0%)	253 (72.1%)	…
45–64	20 (12.5%)	25 (34.7%)	44 (55.7%)	4 (10.0%)	93 (26.5%)	…
65+	0 (0.0%)	5 (6.9%)	0 (0.0%)	0 (0.0%)	5 (1.4%)	…
Sex						.12
Female	84 (52.5%)	31 (43.1%)	34 (43.0%)	25 (62.5%)	174 (49.6%)	…
Male	76 (47.5%)	41 (56.9%)	45 (57.0%)	15 (37.5%)	177 (50.4%)	…
Race						.15
White	95 (59.4%)	50 (69.4%)	47 (59.5%)	22 (55.0%)	214 (61.0%)	…
Hispanic or Latino	30 (18.8%)	10 (13.9%)	22 (27.8%)	5 (12.5%)	67 (19.1%)	…
Black	14 (8.8%)	7 (9.7%)	5 (6.3%)	7 (17.5%)	33 (9.4%)	…
Asian or Pacific Islander	11 (6.9%)	3 (4.2%)	2 (2.5%)	5 (12.5%)	21 (6.0%)	…
Other	10 (6.2%)	2 (2.8%)	3 (3.8%)	1 (2.5%)	16 (4.6%)	…
severity						<.01
Asymptomatic	3 (1.9%)	1 (1.4%)	0 (0.0%)	0	4 (1.3%)	…
Outpatient	147 (91.9%)	61 (84.7%)	58 (73.4%)	0	266 (85.5%)	…
Hospitalized	10 (6.2%)	10 (13.9%)	21 (26.6%)	0	41 (13.2%)	…
Charlson comorbidity index						<.01
0	160 (100.0%)	45 (62.5%)	44 (55.7%)	40 (100.0%)	289 (82.3%)	…
1–2	0 (0.0%)	19 (26.4%)	29 (36.7%)	0 (0.0%)	48 (13.7%)	…
3–4	0 (0.0%)	5 (6.9%)	6 (7.6%)	0 (0.0%)	11 (3.1%)	…
5+	0 (0.0%)	3 (4.2%)	0 (0.0%)	0 (0.0%)	3 (0.9%)	…
Body mass index						<.01
Normal (≤24.9 kg/m^2)	113 (70.6%)	16 (22.9%)	9 (11.8%)	8 (22.2%)	146 (42.7%)	
Overweight (25–29.9 kg/m^2)	17 (10.6%)	22 (31.4%)	26 (34.2%)	13 (36.1%)	78 (22.8%)	
Obese (30–39.9 kg/m^2)	20 (12.5%)	20 (28.6%)	24 (31.6%)	9 (25.0%)	73 (21.3%)	
Severely obese (≥40 kg/m^2)	10 (6.2%)	12 (17.1%)	17 (22.4%)	6 (16.7%)	45 (13.2%)	

Downloaded from academic.oup.com/jid/article/234/4/e869/8713052 by guest on 18 October 2026

Table 1. Continued

	Participants With ML Symptom-based Phenotyping[a] (N = 160)	Participants With Cognitive Phenotyping (BRACE[b]) (N = 72)	Participants With Cardiopulmonary Phenotyping (ChIPS[c]) (N = 79)	Controls (N = 40)	Total (N = 351)	*P* Value[d]
Variant: primary infection[e]						<.01
Alpha	22 (13.8%)	2 (2.8%)	9 (11.4%)	…	33 (10.6%)	
Ancestral	84 (52.5%)	2 (2.8%)	36 (45.6%)	…	122 (39.2%)	
Delta[f]	34 (21.2%)	42 (58.3%)	25 (31.6%)	…	101 (32.5%)	
Omicron[g]	20 (12.5%)	26 (36.1%)	9 (11.4%)	…	55 (17.7%)	
Time between first COVID-19 positive to whole-blood sample collection						<.01
Median (SD)	31 (15.3)	39 (44.8)	29 (15)	…	32 (27.3)	
Range	0.0–59.0	6.0–259.0	1.0–53.0	…	0.0–259.0	
Time between enrollment to whole-blood sample collection[h]						
Median (SD)	…	…	…	0 (14.3)	0 (14.3)	
Range	…	…	…	0.0–36.0	0.0–36.0	
Military status						<.01
Active duty	120 (75.0%)	37 (51.4%)	37 (46.8%)	24 (60.0%)	218 (62.1%)	
Dependent	36 (22.5%)	19 (26.4%)	20 (25.3%)	13 (32.5%)	88 (25.1%)	
Retired military	4 (2.5%)	16 (22.2%)	22 (27.8%)	3 (7.5%)	45 (12.8%)	
DOW[i] affiliation						.03
Air force	20 (12.5%)	10 (13.9%)	24 (30.4%)	2 (5.0%)	56 (16.0%)	
Army	81 (50.6%)	40 (55.6%)	33 (41.8%)	17 (42.5%)	171 (48.7%)	
Navy	43 (26.9%)	16 (22.2%)	16 (20.3%)	18 (45.0%)	93 (26.5%)	
Coast guard	2 (1.2%)	1 (1.4%)	1 (1.3%)	0 (0.0%)	4 (1.1%)	
Marines	9 (5.6%)	2 (2.8%)	5 (6.3%)	3 (7.5%)	19 (5.4%)	
National guard	1 (0.6%)	1 (1.4%)	0 (0.0%)	0 (0.0%)	2 (0.6%)	
Other	3 (1.9%)	0 (0.0%)	0 (0.0%)	0 (0.0%)	3 (0.9%)	
Public health service	1 (0.6%)	2 (2.8%)	0 (0.0%)	0 (0.0%)	3 (0.9%)	

[a]ML: machine learning.

[b]BRACE: Brain Baseline Assessment of Cognition and Everyday Functioning.

[c]ChIPS: Chronic Impairment with Pulmonary Symptoms study module with included 6-minute-walk-test.

[d]*N* × *k* Fisher's exact test. *P* values were not calculated where data were not available for one or more groups.

[e]Variant determined by the temporal context of the primary infection.

[f]Based on infection date 1 July 2021 to 31 December 2021.

[g]Based on infection date 1 January 2022 to 31 May 2022.

[h]Participants with no history of SARS-CoV-2 infection.

[i]Department of War.

Downloaded from academic.oup.com/jid/article/234/4/e869/8713052 by guest on 18 October 2026

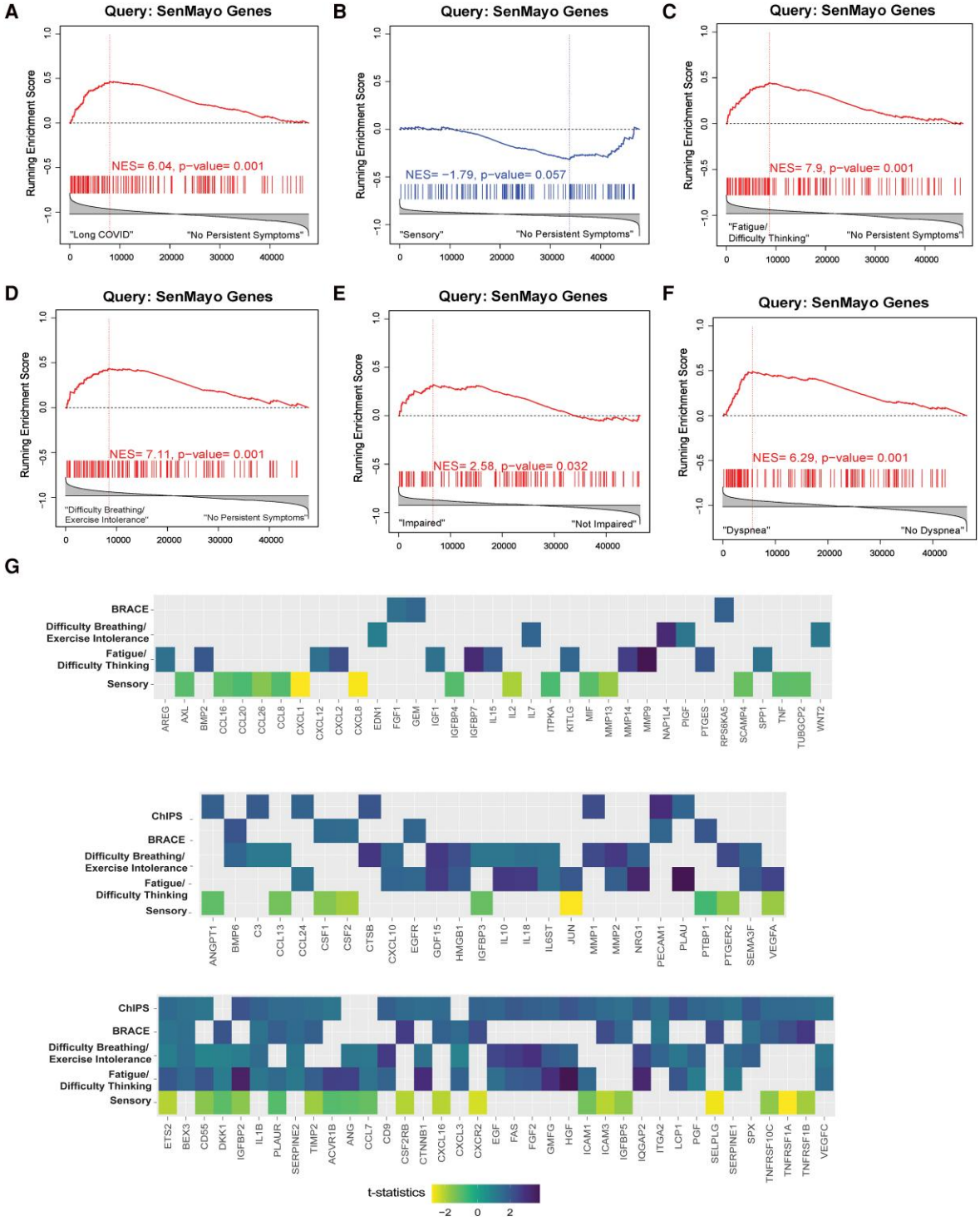


Figure 1. Differential gene set enrichment analysis (GSEA) of SenMayo gene set (measured early postinfection) across Long COVID phenotypes. *A*, Participants who subsequently reported any moderate–severe symptoms at 3–9 m ("Long COVID") versus those who did not report any moderate–severe symptoms at 3–9 m symptoms ("No Persistence Symptoms"), (*B-D*) GSEA of machine learning (ML)-based symptom groups (sensory, fatigue/difficulty thinking, and difficulty breathing/exercise intolerance) at 3–9 m versus participants without moderate-to-severe symptoms at 3–9 m, (*E*) Participants with chronic objective cognitive impairment ("Impaired") versus those without impairment ("Not Impaired"), (*F*) Participants with chronic dyspnea ("Dyspnea") versus those without chronic dyspnea ("No Dyspnea"), note that chronic dyspnea correlated with objective 6-minute-walk-test decrement; plots display normalized enrichment scores (NES) and associated *P* values. *G*, Heatmap display genes across different Long COVID phenotypes: ML-based symptom clusters (Sensory, Fatigue/Difficulty thinking, and Difficulty breathing/Exercise Intolerance), cognitive impairment (BRACE), and cardiopulmonary impairment (ChIPS). Cooler colors (dark blue) indicate upregulation and warmer color (yellow) indicate downregulation relative to acute COVID comparators. Top panel shows BRACE and symptom phenotypes only, as no distinct leading-edge genes were observed in ChIPS for that subset. Middle and bottom panels further illustrate gene overlaps and distinctions across phenotypes.

Downloaded from academic.oup.com/jid/article/234/4/e869/8713052 by guest on 18 October 2026

with cognitive issues such as brain fog; difficulty breathing/exercise intolerance (n = 27), dominated by respiratory symptoms; and no symptoms (n = 104), comprising participants without Long COVID symptoms at 3–9 months postinfection (Supplementary Table 3). COVID-19 hospitalization was more common in fatigue/difficulty thinking cluster (35%) than in other clusters (0% to 15%). No significant differences in age group, sex, or race were observed across the clusters. Blood sample collection timing was similar across all groups though the range is wide.

The BRACE substudy (Supplementary Table 4) investigated cognitive outcomes at a median of 9 months among participants (n = 72) with a history of SARS-CoV-2 infection, comparing those with and without cognitive impairment. Participants with a history of SARS-CoV-2 infection who had RNA-seq data were retained for this analysis. No significant differences in the timing of postinfection blood sample collection were found between those with and without cognitive impairment. However, younger age and female sex were more common with BRACE impairment in this dataset.

In the ChIPS substudy (Supplementary Table 5), 79 participants with early RNA sequencing with and without chronic dyspnea at 3 months postinfection were compared. Hospitalization was more frequent in the dyspnea group (42.3%) compared with no dyspnea (18.9%). Assessments showed that participants with dyspnea had shorter 6MWT distances (1300 ± 247.4 feet vs 1400 ± 425.6 feet). No significant differences were observed in sex between the 2 groups. Severe obesity was more common in those with dyspnea (41.7%) compared with 13.5% of those without dyspnea.

Transcriptomic Signatures in Long COVID

ML-based Symptom Phenotypes

Transcriptomic analyses revealed significant enrichment of the SenMayo gene set in the ML-based symptom phenotyping analysis (Figure 1*A-D*). Participants who reported any symptoms at 3–9 months post-SARS-CoV-2 infection showed strong upregulation of the SenMayo signature (NES = 6.04, $P = .001$) (Figure 1*A*), with top leading-edge genes including *IQGAP2*, *GDF15*, *GMFG*, *FGF2*, and *EGF*.

When stratified by symptom-defined clusters (Figure 1*B-D*), individuals in fatigue/difficulty thinking cluster (NES = 7.9, $P = .001$) showed prominent upregulation of *HGF*, *IGFBP2*, *MMP9*, *PLAU*, and *IQGAP2*. Difficulty breathing/exercise intolerance cluster (NES = 7.11, $P = .001$) was enriched for *NAP1L4*, *FGF2*, *CD9*, *FAS*, and *EGF*. In contrast, those with sensory symptoms (eg, anosmia and ageusia) demonstrated a trend toward downregulation (NES = −1.79, $P = .057$), with lower expression of *JUN*, *TNFRSF1A*, *CXCL1*, *CXCL8*, and *SELPLG*, suggesting a biological distinct phenotype.

We further validated these findings by comparing phenotypes in negative-control participants who had not been infected with SARS-CoV-2 at the time of whole-blood collection. A similar pattern was observed (Supplementary Figure 4A-C): SenMayo gene expression was significantly upregulated in fatigue/difficulty thinking (NES = 6.84, $P = .001$) and difficulty breathing/exercise intolerance (NES = 6.2, $P = .001$) clusters, but downregulated in sensory cluster (NES = −2.5, $P = .007$), suggesting a biologically distinct phenotype.

Objectively Measured Cognitive Phenotype

In the BRACE substudy, participants with cognitive impairment at a median of 9 months postinfection demonstrated modest enrichment of the SenMayo gene set compared with those without impairment (NES = 2.58, $P = .032$) (Figure 1*E*). Top 5 leading-edge genes contributing to this enrichment included *TNFRSF1B*, *CSF2RB*, *ICAM3*, *SELPLG*, and *CXCR2*, several of which are associated with neuroinflammation and immune signaling.

However, when compared with the uninfected control group (Supplementary Figure 4D-E), neither the impaired nor the unimpaired participants showed statistically significant enrichment. The impaired group showed upregulation (NES = 1.52, $P = .25$), while the nonimpaired group showed a nonsignificant downregulation (NES = −1.09, $P = .42$). Furthermore, in sensitivity analyses restricted to samples collected within a defined postinfection time window, the enrichment signal did not remain statistically significant (Supplementary Figure 4H).

Cardiopulmonary Outcomes

In the cardiopulmonary Outcomes (ChIPS) substudy, the SenMayo gene set was significantly enriched in participants with chronic dyspnea at 3 months postinfection compared with those without dyspnea (NES = 6.29, $P = .001$) (Figure 1*F*). Leading-edge genes driving this enrichment included *PECAM1*, *LCP1*, *IGFBP2*, *HGF*, and *SPX*.

When compared with the uninfected control group (Supplementary Figure 4F-G), participants with chronic dyspnea also demonstrated significant upregulation of the SenMayo gene set (NES = 6.05, $P = .001$). Participants without dyspnea showed no significant enrichment (NES = 2.19, $P = .093$). Enrichment remained statistically significant in sensitivity analyses restricted to participants without severe obesity and without prior hospitalization (Supplementary Figure 4I).

Comparative Analysis Across Long COVID Phenotypes

Comparative transcriptomic analyses across all Long COVID phenotypes revealed both shared and distinct SenMayo gene expression patterns (Figure 1*G*; Supplementary Figure 5). Some genes, such as *ETS2*, were expressed across all phenotypes, indicating a shared senescence-related response. Other genes displayed phenotype-specific variability, for example *MMP2*, *IL10*, *IL18*, *IL6ST*, *NRG1*, and *CXCL10* were upregulated in both fatigue/difficulty thinking and difficulty

Downloaded from academic.oup.com/jid/article/234/4/e869/8713052 by guest on 18 October 2026

breathing/exercise intolerance clusters. In contrast, *BEX3*, *IL1B*, and *SERPINE2* were elevated in all phenotypes except sensory. Genes such as *CSF2RB*, *CXCL16*, *CXCR2*, *ICAM3*, *IGFBP5*, and *TNFRSF1A* were expressed in ML-sensory, BRACE (cognitive impairment), and ChIPS (dyspnea) phenotypes but not in fatigue/difficulty thinking and difficulty breathing/exercise intolerance phenotypes. Additionally, *EGF*, *FAS*, *HGF*, and *VEGFC* were commonly upregulated in fatigue/difficulty thinking, difficulty breathing/exercise intolerance, and ChIPS groups. Finally, *ANG* and *CCL7* were uniquely expressed in the ML-based symptom-based phenotypes.

Immune Cell Deconvolution Reveals Phenotype-specific Signatures

To better understand the cellular context of transcriptomic changes, we performed immune cell deconvolution analysis, which revealed distinct phenotype-specific patterns (Supplementary Figure 6). Participants in fatigue/difficulty thinking cluster exhibited transcriptomic findings consistent with reduced $CD4^+$ T cells and elevated endothelial cells (likely reflecting endothelial-derived transcripts detected in peripheral blood) compared with those in sensory, difficulty breathing/exercise intolerance, no Long COVID symptoms, and control groups. In contrast, individuals with cognitive impairment in the BRACE substudy showed increased $CD4^+$ T-cells frequencies compared with the cognitively not impaired and control groups. In the ChIPS dyspnea cohort, elevated B cells and $CD4^+$ T cells were observed compared with those without dyspnea and in the uninfected control group.

Robustness and Specificity Analyses of SenMayo Enrichment Across Long COVID Phenotypes

To further evaluate the robustness and specificity of these findings, we performed GSEA using established inflammatory gene sets (Hallmark TNF-alpha Signaling via NF-kB; Hallmark IL-6/JAK/STAT3 Signaling; Hallmark Interferon-Gamma Response). This demonstrated comparable or greater enrichment across several phenotypes, indicating substantial overlap between senescence-associated and broader inflammatory transcriptional programs (Supplementary Figure 7A).

Finally, FDR correction across all GSEA comparisons yielded results consistent with nominal *P* values, and adjustment for EPIC-derived cell proportion did not materially alter the observed enrichment patterns (Supplementary Figure 7B).

DISCUSSION

This study identified enrichment of senescence-associated transcriptional signatures derived from the SenMayo gene set across multiple Long COVID phenotypes within a cohort of MHS beneficiaries. Our analyses underscore the heterogeneity of gene expression signatures associated with different Long COVID-19 phenotypes. This heterogeneity may be due, in part, to true biological differences of pathogenesis underlying different Long COVID phenotypes, but it may also be driven by differences in how Long COVID is measured and defined, differences in cell populations, and/or other causes of transcriptomic "noise," which is inherent in bulk transcriptomic analysis. Still, our results highlight both shared and unique candidate molecular genes underpinning varying forms of Long COVID and prompt further mechanistic study, which may offer further insights into its pathogenesis and potential therapeutic targets.

While these findings are consistent with enrichment of senescence-associated transcriptional programs, they should not be interpreted as definitive evidence of cellular senescence. SenMayo enrichment may reflect a combination of senescence-associated biology and postinfectious immune activation, as parallel GSEA using established inflammatory Hallmark gene sets demonstrated comparable, and in some cases stronger enrichment. Notably, sensory phenotype showed relative downregulation of SenMayo-associated signatures, in contrast to the enrichment observed in other phenotypes. This heterogeneity suggests that Long COVID may comprise biologically distinct subtypes with differing contributions from senescence-associated and inflammatory pathways. Together, these findings highlight the close interplay between senescence-associated and broader inflammatory transcriptional programs [36].

We observed increased *ETS2* expression across multiple Long COVID phenotypes, whereas the sensory phenotype demonstrated relative downregulation of ETS2. Evidence for ETS2 enrichment was also attenuated in some BRACE sensitivity analyses. ETS2 has been described as a broadly acting transcription factor [37] involved in inflammatory signaling, macrophage function [38] and endothelial activation [39] and is inducible by viral and inflammatory stimuli [40]. Therefore, its upregulation in whole blood may represent a shared inflammatory regulatory node rather than a senescence-specific marker, highlighting the overlap between senescence-associated and broader immune activation pathways.

Other gene expression profiles were shared across smaller numbers of phenotypes, or individual phenotypes. For example, in fatigue/difficulty thinking ML-based phenotype, *MMP9* was elevated, and this gene has been linked to Long COVID symptom severity, neurologic involvement, and blood–brain barrier disruption, suggesting a potential role in post-COVID cognitive and inflammatory symptoms [41]. In addition, the High Mobility Group Box 1 (*HMGB1*), a nuclear protein and proinflammatory damage-associated molecular pattern molecule [42] known as a neuroinflammation marker [43], was significantly elevated in the fatigue/difficulty thinking and difficulty breathing/exercise intolerance phenotype, which may align with its known role in lung dysfunction and chronic

Downloaded from academic.oup.com/jid/article/234/4/e869/8713052 by guest on 18 October 2026

inflammation [44, 45]. Hepatocyte growth factor (*HGF*), a pleiotropic protein involved in tissue repair, angiogenesis, inflammation, and fibrosis was elevated in cardiopulmonary (ChIPS), fatigue/difficulty thinking, and difficulty breathing/exercise intolerance phenotypes [46]. Taken together, these differences in transcriptomic signatures across different phenotypes suggest that Long COVID is unlikely to represent a single unified senescence-driven process and instead may comprise multiple biologically distinct subtypes with differing contribution from senescence-associated and inflammatory pathways. These findings highlight the importance of phenotype-specific investigations when studying Long COVID biology.

Several limitations should be acknowledged. First, bulk transcriptomic analyses are influenced by cellular composition, and although adjustment using EPIC-derived cell proportion estimates did not materially alter enrichment patterns, residual confounding cannot be excluded. Additional validation using quantitative PCR, PBMC-based senescence markers, or single-cell RNA sequencing could strengthen these findings. Furthermore, while the SenMayo gene set is a validated measure of senescence-associated transcriptional programs, it may not fully distinguish cellular senescence from post-infectious inflammation, which are closely interconnected processes [36].

A further limitation is that the SenMayo gene set was developed and validated in nonblood tissues, although SenMayo has been used in peripheral blood analyses of other senescence-associated tissue specific disorders (eg, breast cancer [47] and myeloma [48]). Interpretation of circulating senescence-associated signatures remains uncertain. In whole blood, enrichment of SenMayo genes may reflect systemic immune activation, shifts in immune cell composition, or inflammatory responses occurring secondary to tissue injury rather than directly measuring tissue-level senescent cells burden. Therefore, the observed enrichment should be interpreted as evidence of senescence-associated transcriptional programs in circulation rather than definitive evidence of senescent cell accumulation within specific tissues.

Timing of blood sampling is also a limitation of this analysis. The single time point design limited discrimination of persistent senescence-associated biology from delayed resolution of postinfectious inflammation and BRACE sensitivity analyses restricted to a narrower early postinfection window attenuated the observed enrichment. Other sensitivity analyses also attenuated BRACE findings, suggesting that the cognitive impairment findings should be considered exploratory and hypothesis-generating pending validation in independent cohort, particularly as BRACE is a screening tool. Finally, we employed multiple classification approaches, incorporating both subjective symptom reports and objective phenotyping. This led to differences in participant characteristics between the Long COVID phenotyping approaches, which could have influenced observed transcriptomic differences across the phenotypes. For example, symptom-cluster analyses were restricted by age and excluded participants with prior comorbidities, and hospitalization rates differed between phenotypes.

Taken together, these results open potential avenues for additional studies. Interventions targeting senescence-associated [49] and inflammatory pathways may hold promises for mitigating the effects of Long COVID. Early identification of at-risk individuals through senescence-related transcriptional biomarkers, interpreted within the caveats and limitations of the current analysis, could enable targeted treatments interventions aimed at reducing senescence burden and improving recovery.

Supplementary Data

Supplementary materials are available at *The Journal of Infectious Diseases* online (http://jid.oxfordjournals.org/). Supplementary materials consist of data provided by the author that are published to benefit the reader. The posted materials are not copyedited. The contents of all supplementary data are the sole responsibility of the authors. Questions or messages regarding errors should be addressed to the author.

Notes

Acknowledgments. The authors wish to also acknowledge all who have contributed to the EPICC COVID-19 study: Alexander T. Augusta Military Medical Center, Fort Belvoir, VA: N. Dimascio-Johnson; N. Elnahas; E. Ewers; K. Gallagher; C. Glinn; U. Jarral; D. Jennings; D. Larson; K. Reterstoff; A. Rutt; A. Silva; C. West. Brooke Army Medical Center, Fort Sam Houston, TX: J. Cowden; M. Darling; S. DeLeon; D. Lindholm; A. Markelz; K. Mende; S. Merritt; T. Merritt; N. Turner T. Wellington. Carl R. Darnall Army Medical Center, Fort Hood, TX: S. Bazan; P.K Love. Digital Artefacts, Iowa City IA: Severson, J. John Hopkins University School of Medicine, Baltimore, MD: Rubin. L. Henry M. Jackson Foundation, Inc., Bethesda, MD: P. Blair; J. Chenoweth; D. Clark. Madigan Army Medical Center, Joint Base Lewis McChord, WA: J. Bowman; S. Chambers; C. Colombo; R. Colombo; C. Conlon; K. Everson; P. Faestel; T. Ferguson; L. Gordon; S. Grogan; S. Lis; M. Martin; C. Mount; D. Musfeldt; D. Odineal; M. Perreault; W. Robb-McGrath; R. Sainato; C. Schofield; C. Skinner; M. Stein; M. Switzer; M. Timlin; S. Wood. Naval Medical Center Portsmouth, Portsmouth, VA: S. Banks; R. Carpenter; L. Kim; K. Kronmann; T. Lalani; T. Lee; A. Smith; R. Smith; R. Tant; T. Warkentien. Naval Medical Center San Diego, San Diego, CA: C. Berjohn; S. Cammarata; N. Kirkland; D. Libraty; R. Maves; G. Utz. Tripler Army Medical Center, Honolulu, HI: C. Bradley; S. Chi;

Downloaded from academic.oup.com/jid/article/234/4/e869/8713052 by guest on 18 October 2026

R. Flanagan; A. Fuentes; M. Jones; N. Leslie; C. Lucas; C. Madar; K. Miyasato; C. Uyehara. Uniformed Services University of the Health Sciences, Bethesda, MD: H. Adams; B. Agan; L. Andronescu; A. Austin; B. Barton, D. Becher, C. Broder; T. Burgess; C. Byrne; K Chung; J. Davies; C. English; N. Epsi; C. Fox; M. Fritschlanski; A. Hadley; P. Hickey; E. Laing; C. Lanteri; J. Livezey; A. Malloy; A. Michel, R. Mohammed; C. Morales; P. Nwachukwu; C. Olsen; E. Parmelee; S. Pollett; S. Richard; J. Rothenberg, J. Rozman; J. Rusiecki; D. Saunders; E. Samuels; M. Sanchez; A. Scher; M. Simons; A. Snow; K. Telu; D. Tribble; M. Tso; L. Ulomi; M. Wayman, N. Hockenbury. United States Air Force School of Aerospace Medicine, Dayton, OH: T. Chao; R. Chapleau; M. Christian; A. Fries; C. Harrington; V. Hogan; S. Huntsberger; K. Lanter; E. Macias; J. Meyer; S. Purves; K. Reynolds; J. Rodriguez; C. Starr. United States Coast Guard, Washington, DC: J. Iskander; I. Kamara. Womack Army Medical Center, Fort Bragg, NC: B. Barton; D. Hostler; J. Hostler; K. Lago; C. Maldonado; J. Mehrer. William Beaumont Army Medical Center, El Paso, TX: T. Hunter; J. Mejia; R. Mody; J. Montes; R. Resendez; P. Sandoval. Walter Reed National Military Medical Center, Bethesda, MD: I. Barahona; A. Baya; A. Ganesan; N. Huprikar; B. Johnson. Walter Reed Army Institute of Research, Silver Spring, MD: S. Peel

Financial support. This work was supported by awards from the Defense Health Program, U.S. Department of War (HU00012020067) and the National Institute of Allergy and Infectious Disease (HU00012120103). The protocol was executed by the Infectious Disease Clinical Research Program (IDCRP), a Department of War (DoW) program executed by the Uniformed Services University of the Health Sciences (USUHS) through a cooperative agreement by the Henry M. Jackson Foundation for the Advancement of Military Medicine, Inc. (H. J. F). This project has been funded in part by the National Institute of Allergy and Infectious Diseases at the National Institutes of Health, under an interagency agreement (Y1-AI-5072).

Data Availability. Data for this study are available from the Infectious Disease Clinical Research Program (IDCRP), headquartered at the Uniformed Services University of the Health Sciences (USU), Department of Preventive Medicine and Biostatistics. Review by the USU Institutional Review Board is required for use of the data collected under this protocol. Furthermore, the data set includes Military Health System data collected under a Data Use Agreement that requires accounting for uses of the data. Data requests may be sent to: Address: 6270A Rockledge Drive, Suite 250, Bethesda, MD 20817. Email: contactus@idcrp.org.

Disclaimer. The contents of this publication are the sole responsibility of the author(s) and do not necessarily reflect the views, opinions, or policies of Uniformed Services University of the Health Sciences (USUHS); the Department of War (DoW); the Departments of the Army, Navy, or Air Force; Brooke Army Medical Center; Walter Reed National Military Medical Center; Madigan Army Medical Center; or the Henry M. Jackson Foundation for the Advancement of Military Medicine. M. J. M., D. A. L., M. U. J., A. M.W. M., D. R. T., T. H. B., and C. D. are service members or employees of the U.S. Government. This work was prepared as part of their official duties. Title 17 U.S.C. §105 provides that "Copyright protection under this title is not available for any work of the United States Government." Title 17 U.S.C. §101 defines a U.S. Government work as a work prepared by a military service member or employee of the U.S. Government as part of that person's official duties. Mention of trade names, commercial products, or organizations does not imply endorsement by the U.S. Government. The investigators have adhered to the policies for protection of human subjects as prescribed in 45 CFR 46.

Potential conflicts of interest. S. D. P., T. H. B., and D. R. T. report that the Uniformed Services University (USU) Infectious Diseases Clinical Research Program (IDCRP), a US Department of War institution, and the Henry M. Jackson Foundation (HJF) were funded under a Cooperative Research and Development Agreement to conduct an unrelated phase III COVID-19 monoclonal antibody immunoprophylaxis trial sponsored by AstraZeneca. The HJF, in support of the USU IDCRP, was funded by the Department of War Joint Program Executive Office for Chemical, Biological, Radiological, and Nuclear Defense to augment the conduct of an unrelated phase III vaccine trial sponsored by AstraZeneca. Both of these trials were part of the US Government COVID-19 response. Neither is related to the work presented here.

All authors have submitted the ICMJE Form for Disclosure of Potential Conflicts of Interest. Conflicts that the editors consider relevant to the content of the manuscript have been disclosed.

References

1. National Academies of Sciences, Engineering, and Medicine; Health and Medicine Division; Board on Global Health; Board on Health Sciences Policy; Committee on Examining the Working Definition for Long COVID. A long COVID definition: a chronic, systemic disease state with profound consequences. Washington, DC: The National Academies Press, **2024**.
2. Cox LS, Bellantuono I, Lord JM, et al. Tackling immunosenescence to improve COVID-19 outcomes and vaccine response in older adults. Lancet Healthy Longev **2020**; 1: e55–7.
3. Chen Y, Klein SL, Garibaldi BT, et al. Aging in COVID-19: vulnerability, immunity and intervention. Ageing Res Rev **2021**; 65:101205.

Downloaded from academic.oup.com/jid/article/234/4/e869/8713052 by guest on 18 October 2026

4. Nehme J, Borghesan M, Mackedenski S, Bird TG, Demaria M. Cellular senescence as a potential mediator of COVID-19 severity in the elderly. Aging Cell **2020**; 19: e13237.
5. Gorgoulis V, Adams PD, Alimonti A, et al. Cellular senescence: defining a path forward. Cell **2019**; 179:813–27.
6. Rovillain E, Mansfield L, Lord CJ, Ashworth A, Jat PS. An RNA interference screen for identifying downstream effectors of the p53 and pRB tumour suppressor pathways involved in senescence. BMC Genomics **2011**; 12:355.
7. Kobashigawa S, Sakaguchi YM, Masunaga S, Mori E. Stress-induced cellular senescence contributes to chronic inflammation and cancer progression. Therm Med **2019**; 35:41–58.
8. Liu X, Wan M. A tale of the good and bad: cell senescence in bone homeostasis and disease. Int Rev Cell Mol Biol **2019**; 346:97–128.
9. Takasugi M, Yoshida Y, Ohtani N. Cellular senescence and the tumour microenvironment. Mol Oncol **2022**; 16: 3333–51.
10. Chambers CR, Ritchie S, Pereira BA, Timpson P. Overcoming the senescence-associated secretory phenotype (SASP): a complex mechanism of resistance in the treatment of cancer. Mol Oncol **2021**; 15:3242–55.
11. Campisi J. Aging, cellular senescence, and cancer. Annual Rev Physiol **2013**; 75:685–705.
12. Herranz N, Gil J. Mechanisms and functions of cellular senescence. J Clin Invest **2018**; 128:1238–46.
13. Campisi J, d'Adda di Fagagna F. Cellular senescence: when bad things happen to good cells. Nat Rev Mol Cell Biol **2007**; 8:729–40.
14. Liu Z, Liang Q, Ren Y, et al. Immunosenescence: molecular mechanisms and diseases. Signal Transduct Target Ther **2023**; 8:200.
15. Prata L, Ovsyannikova IG, Tchkonia T, Kirkland JL. Senescent cell clearance by the immune system: emerging therapeutic opportunities. Semin Immunol **2018**; 40:101275.
16. Nikolich-Zugich J. Ageing and life-long maintenance of T-cell subsets in the face of latent persistent infections. Nat Rev Immunol **2008**; 8:512–22.
17. Saul D, Kosinsky RL, Atkinson EJ, et al. A new gene set identifies senescent cells and predicts senescence-associated pathways across tissues. Nat Commun **2022**; 13:4827.
18. Tchkonia T, Zhu Y, van Deursen J, Campisi J, Kirkland JL. Cellular senescence and the senescent secretory phenotype: therapeutic opportunities. J Clin Invest **2013**; 123:966–72.
19. Schmitt CA, Tchkonia T, Niedernhofer LJ, Robbins PD, Kirkland JL, Lee S. COVID-19 and cellular senescence. Nat Rev Immunol **2023**; 23:251–63.
20. Lee S, Yu Y, Trimpert J, et al. Virus-induced senescence is a driver and therapeutic target in COVID-19. Nature **2021**; 599:283–9.
21. Group P-CC. Clinical characteristics with inflammation profiling of long COVID and association with 1-year recovery following hospitalisation in the UK: a prospective observational study. Lancet Respir Med **2022**; 10:761–75.
22. Talla A, Vasaikar SV, Szeto GL, et al. Persistent serum protein signatures define an inflammatory subcategory of long COVID. Nat Commun **2023**; 14:3417.
23. Davis HE, McCorkell L, Vogel JM, Topol EJ. Long COVID: major findings, mechanisms and recommendations. Nat Rev Microbiol **2023**; 21:133–46.
24. Richard SA, Pollett SD, Lanteri CA, et al. COVID-19 Outcomes among US Military Health System beneficiaries include complications across multiple organ systems and substantial functional impairment. Open Forum Infect Dis **2021**; 8:ofab556.
25. Epsi NJ, Richard SA, Lindholm DA, et al. Understanding "Hybrid Immunity": comparison and predictors of humoral immune responses to Severe Acute Respiratory Syndrome Coronavirus 2 Infection (SARS-CoV-2) and Coronavirus Disease 2019 (COVID-19) vaccines. Clin Infect Dis **2023**; 76:e439–49.
26. Richard SA, Epsi NJ, Pollett S, et al. Performance of the inFLUenza Patient-Reported Outcome Plus (FLU-PRO Plus) instrument in patients with coronavirus disease 2019. Open Forum Infect Dis **2021**; 8:ofab517.
27. Epsi NJ, Chenoweth JG, Blair PW, et al. Precision symptom phenotyping identifies early clinical and proteomic predictors of distinct COVID-19 sequelae. J Infect Dis **2025**; 232: 39–49.
28. Andronescu L, Richard SA, Hone E, et al. 387. understanding the impact of COVID-19 on cognitive function using a scalable, app-based, self-administered tool in the military. Open Forum Infect Dis **2023**; 10:ofad500.457.
29. Goertzen SM, Lindholm DA, Walter RJ, et al. Clinical, radiographic, and physiological correlates of post-COVID-19 dyspnea in military health system beneficiaries: results from the Chronic Impairment With Pulmonary Symptoms (ChIPS) sub-study. Open Forum Infect Dis **2025**; 12:ofaf633.
30. Thaweethai T, Jolley SE, Karlson EW, et al. Development of a definition of postacute sequelae of SARS-CoV-2 infection. JAMA **2023**; 329:1934–46.
31. Andronescu LR, Richard SA, Scher AI, et al. SARS-CoV-2 infection is associated with self-reported post-acute neuropsychological symptoms within six months of follow-up. PLoS One **2024**; 19:e0297481.
32. Love MI, Huber W, Anders S. Moderated estimation of fold change and dispersion for RNA-Seq data with DESeq2. Genome Biol **2014**; 15:550.
33. Racle J, Gfeller D. EPIC: a tool to estimate the proportions of different cell types from bulk gene expression data. Meth Mol Biol (Clifton, NJ) **2020**; 2120:233–48.

Downloaded from academic.oup.com/jid/article/234/4/e869/8713052 by guest on 18 October 2026

34. Subramanian A, Tamayo P, Mootha VK, et al. Gene set enrichment analysis: a knowledge-based approach for interpreting genome-wide expression profiles. Proc Natl Acad Sci U S A **2005**; 102:15545–50.
35. Team TRDC. R: a language environment for statistical computing. Vienna, Austria: R Foundation for Statistical Computing, **2020**.
36. Camell CD, Yousefzadeh MJ, Zhu Y, et al. Senolytics reduce coronavirus-related mortality in old mice. Science (New York, NY) **2021**; 373:eabe4832.
37. Hsu T, Trojanowska M, Watson DK. Ets proteins in biological control and cancer. J Cell Biochem **2004**; 91: 896–903.
38. Stankey CT, Bourges C, Haag LM, et al. A disease-associated gene desert directs macrophage inflammation through ETS2. Nature **2024**; 630:447–56.
39. Cheng C, Tempel D, Den Dekker WK, et al. Ets2 determines the inflammatory state of endothelial cells in advanced atherosclerotic lesions. Circ Res **2011**; 109:382–95.
40. Ma X, Jiang Z, Li N, et al. Ets2 suppresses inflammatory cytokines through MAPK/NF-κB signaling and directly binds to the IL-6 promoter in macrophages. Aging **2019**; 11:10610–25.
41. Kempuraj D, Tsilioni I, Aenlle KK, Klimas NG, Theoharides TC. Long COVID elevated MMP-9 and release from microglia by SARS-CoV-2 spike protein. Transl Neurosci **2024**; 15:20220352.
42. Chen R, Kang R, Tang D. The mechanism of HMGB1 secretion and release. Exp Mole Med **2022**; 54:91–102.
43. Mao D, Zheng Y, Xu F, Han X, Zhao H. HMGB1 in nervous system diseases: a common biomarker and potential therapeutic target. Front Neurol **2022**; 13:1029891.
44. Wang M, Gauthier A, Daley L, et al. The role of HMGB1, a nuclear damage-associated molecular pattern molecule, in the pathogenesis of lung diseases. Antioxid Redox Signal **2019**; 31:954–93.
45. Ding J, Cui X, Liu Q. Emerging role of HMGB1 in lung diseases: friend or foe. J Cell Mol Med **2017**; 21:1046–57.
46. Morishita R, Aoki M, Yo Y, Ogihara T. Hepatocyte growth factor as cardiovascular hormone: role of HGF in the pathogenesis of cardiovascular disease. Endocr J **2002**; 49:273–84.
47. Carroll JE, Crespi CM, Cole S, Ganz PA, Petersen L, Bower JE. Transcriptomic markers of biological aging in breast cancer survivors: a longitudinal study. J Natl Cancer Inst **2025**; 117:312–21.
48. Lehoczki A, Menyhart O, Andrikovics H, et al. Prognostic impact of a senescence gene signature in multiple myeloma. GeroScience **2025**; 47:5025–37.
49. Kirkland JL, Tchkonia T. Senolytic drugs: from discovery to translation. J Intern Med **2020**; 288:518–36.

Downloaded from academic.oup.com/jid/article/234/4/e869/8713052 by guest on 18 October 2026